PAPER

Performance Evaluation of Multi-Rate DS-CDMA Using Frequency-Domain Equalization in a Frequency-Selective Fading Channel

Kazuaki TAKEDA[†a)], ***Student Member and*** **Fumiyuki ADACHI**[†], ***Member***

SUMMARY Joint frequency-domain equalization (FDE) and antenna diversity combining is applied to the reception of multi-rate DS-CDMA signals to achieve the frequency diversity effect while suppressing inter-path interference (IPI) resulting from the asynchronism of different propagation paths. At a receiver, fast Fourier transform (FFT) is applied for FDE and then inverse FFT (IFFT) is used to obtain a frequency-domain equalized DS-CDMA chip sequence for the succeeding despreading operation. An arbitrary spreading factor *SF* can be used for the given value of FFT window size; an extreme case is the nonspread SC system with *SF*=1. This property allows a flexible design of multi-rate DS-CDMA systems. Three types of FDE are considered; minimum mean square error (MMSE) equalization, maximal-ratio combining (MRC) equalization and zero-forcing (ZF) equalization. Matched filter bound analysis for achievable BER performance is presented. The improvement in the BER performance in a frequency-selective Rayleigh fading channel is evaluated by computer simulation. First, we consider the single-user case and compare the BER performances achievable with MMSE, MRC and ZF equalizations. How the fading rate and the spreading factor affect the BER performance is also evaluated. Furthermore, the BER performance comparison between FDE and rake combining is presented for various values of *SF* and also performance comparison between DS-CDMA and SC signal transmissions, both using FDE, is presented. Finally, we extend our evaluation to the multi-user case. Both downlink and uplink are considered and how the BER performances of downlink and uplink differ is discussed.

key words: *DS-CDMA, frequency-domain equalization, frequency-selective fading*

1. Introduction

Recently, there have been tremendous demands for high-speed data transmissions in mobile communications [1]. However, the hostile fading channel is a major obstacle to achieve high-speed data transmissions. Mobile communication channel is composed of many distinct propagation paths having different time delays, resulting in a frequency-selective fading channel [2]. In the frequency-selective fading channel, severe inter-symbol interference (ISI) is produced and the bit error rate (BER) performance is significantly degraded when single carrier (SC) transmission is used without using an advanced equalization technique. Recently, direct sequence code division multiple access (DS-CDMA) is used in cellular mobile communications systems for improving the BER performance of around a few Mbps transmissions [3], where coherent rake combining [4] is applied in order to exploit the frequency-selectivity of the fading channel. However, the rake combiner requires as many fingers (correlators) as the number of resolvable propagation paths so that most of the transmitted signal power can be collected, otherwise significant performance degradation occurs [5], and hence, the complexity of rake combiner increases. Furthermore, large inter-path interference (IPI), resulting from asynchronism among different paths, degrades the BER performance even with ideal rake combining. These pose the limitation to the application of DS-CDMA technique to high speed data transmissions in a severe frequency-selective fading channel.

Recent studies have been shifted from DS-CDMA to multicarrier (MC) transmission techniques to overcome the severe frequency-selectivity of the fading channel [6]–[9]. Much attention has been paid to orthogonal frequency division multiplexing (OFDM) and MC-CDMA. MC-CDMA has been considered a promising candidate for broadband wireless multi-access [10]. MC-CDMA using per-subcarrier one-tap frequency-domain equalization (FDE) provides a much better BER performance than DS-CDMA using rake combining [11]. However, MC transmission has a problem of large peak-to-average power ratio (PAPR). To alleviate the PAPR problem, SC transmission techniques have been looked over again with application of FDE as in MC-CDMA [12]. SC transmission with FDE can overcome the ISI problem arising from the severe frequency-selectivity of the channel as well as the PAPR problem and can achieve a BER performance similar to MC-CDMA.

In next generation mobile communications, a flexible support for low-to-very high rate of data services or multi-rates services is required. In DS-CDMA, multi-rate data transmission can be achieved by changing the number of parallel orthogonal spreading codes in multicode transmission or by simply changing the spreading factor in the single-code transmission. Recently, it was shown [13] that FDE based on minimum mean square error (MMSE) criterion can significantly improve the BER performance of multicode DS-CDMA transmission in a frequency-selective fading channel compared to the conventional rake combining and provides almost the same BER performance as MC-CDMA. At a receiver, fast Fourier transform (FFT) is applied for FDE and then inverse FFT (IFFT) is used to obtain

Manuscript received December 12, 2003.
Manuscript revised September 17, 2004.

[†]The authors are with Dept. of Electrical and Communication Engineering, Graduate School of Engineering, Tohoku University, Sendai-shi, 980-8579 Japan.
a) E-mail: takeda@mobile.ecie.tohoku.ac.jp

DOI: 10.1093/ietcom/e88–b.3.1191

a frequency-domain equalized DS-CDMA chip sequence for the succeeding despreading operation. In Ref. [13], the FFT window size for FDE was assumed to be equal to the spreading factor. If this is applied to the single-code DS-CDMA, as the spreading factor reduces (as the data rate increases), the FFT window size becomes smaller and hence the transmission efficiency reduces due to the insertion of the guard interval (GI). However, it should be pointed out here that the FFT window size should not necessarily be equal to the spreading factor. The same FFT window size can be used irrespective of the spreading factor (i.e., irrespective of data rate). This property allows a flexible design of multi-rate DS-CDMA using single-code transmission.

In this paper, we consider a multi-rate and single-code DS-CDMA signal transmission and present the joint use of FDE and antenna diversity combining to achieve the frequency diversity effect while reducing the adverse effect of IPI. The objective of this paper is to (a) show that FDE can be applied to multi-rate and single-code DS-CDMA with arbitrary spreading factor, (b) derive the mathematical signal expressions after despreading to discuss the residual interchip interference (ICI) and analyze the matched filter bound, (c) give performance comparison between single-code and multi-code transmissions, and (d) discuss the BER performance for the uplink and downlink in a multi-rate and multi-user environment.

Remainder of this paper is organized as follows. Section 2 presents the transmission system model for DS-CDMA with FDE and then, presents how FDE can be jointly used with antenna diversity combining at the receiver. The matched filter bound analysis for the BER performance is presented. In Sect. 3, the achievable BER performance in a frequency-selective Rayleigh fading channel is evaluated by computer simulation. Three types of FDE are considered; MMSE-FDE, maximal-ratio combining (MRC)-FDE and zero-forcing (ZF)-FDE, and their achievable BER performances are compared. The impact of fading rate on the BER performance is discussed. Performance comparison of FDE and rake combining is also presented. In the computer simulation, the performance evaluation for the single-user case is done first and then extended to the multi-user case. In the multi-user case, single-rate and multi-rate transmissions are considered and the uplink and downlink performances are compared. Section 4 offers some conclusions and future work.

2. DS-CDMA with Joint FDE and Antenna Diversity Combining

2.1 Transmission System Model

Transmission system model for DS-CDMA with joint FDE and antenna diversity combining is illustrated in Fig. 1. At the transmitter, the binary data sequence is transformed into the data modulated symbol sequence $d(n)$ and then spread by multiplying with the spreading sequence $c(t)$ having an arbitrary spreading factor, SF. The resulting chip sequence is divided into a sequence of blocks of N_c chips each and then, the last N_g chips of each block is copied as a cyclic prefix and inserted into the guard interval (GI) at the beginning of each block to form a sequence of frames of $N_c + N_g$ chips. Figure 2 illustrates the frame structure. The chip sequence is transmitted over a frequency-selective fading channel and is received by N_r diversity antennas at the receiver. The received chip sequence on each antenna is decomposed by N_c-point FFT into N_c subcarrier components (the terminology "subcarrier" is used for explanation purpose only although subcarrier modulation is not used). Then, joint FDE and antenna diversity combining is carried out and IFFT is applied to obtain the equalized and diversity combined time-domain chip sequence for succeeding despreading and data demodulation.

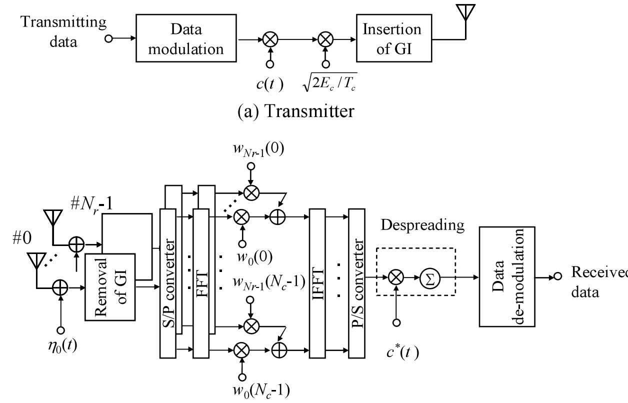

Fig. 1 Transmission system model for DS-CDMA with joint FDE and antenna diversity combining.

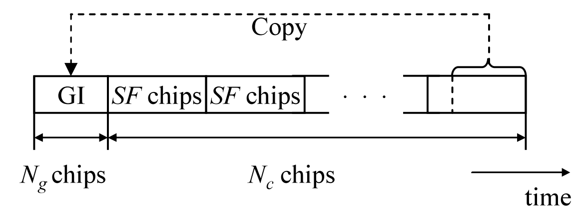

Fig. 2 Frame structure.

2.2 Transmitted and Received Signals Representation

Throughout this paper, the chip-spaced time representation of transmitted signals is used. Without loss of generality, the data symbol sequence $\{d(n);\ n = 0 \sim N_c/SF - 1\}$ and the spreading chip sequence $\{c(t);\ t = 0 \sim SF - 1\}$ of one frame are considered, where $|d(n)| = |c(t)|=1$ and N_c and SF are chosen so that the value of N_c/SF becomes an integer. The GI-inserted chip sequence $\{s(t);\ t = -N_g \sim N_c - 1\}$ can be expressed using the equivalent lowpass representation as

$$s(t) = \sqrt{2E_c/T_c}\, d(\lfloor t/SF \rfloor)\ c(t \bmod SF),\quad t = -N_g \sim N_c - 1, \tag{1}$$

where E_c and T_c denote the chip energy and the chip duration, respectively, and $\lfloor x \rfloor$ represents the largest integer smaller than or equal to x. The propagation channel is assumed to be a frequency-selective fading channel having L discrete paths, each subjected to independent fading, where the time delay τ_l of the lth path ($l = 0 \sim L-1$) is given by $\tau_l = l$ chips. The chip sequence $\{r_m(t);\ m = 0 \sim N_r - 1,\ t = -N_g \sim N_c - 1\}$ received on the mth antenna can be represented as

$$r_m(t) = \sum_{l=0}^{L-1} \xi_{l,m} s(t-l) + \eta_m(t), \tag{2}$$

where $\xi_{l,m}$ is the complex path gain of the lth path experienced at the m-th antenna with $\sum_{l=0}^{L-1} E[|\xi_{l,m}|^2] = 1$ for all m ($E[.]$ denotes the ensemble average operation) and $\eta_m(t)$ is the zero-mean complex noise process having a variance of $2N_0/T_c$ with N_0 being the single-sided power spectrum density of the additive white Gaussian noise (AWGN) process. We have assumed a block fading, where the path gains stay constant over the duration of one frame; however, the BER dependency on the fading rate is evaluated by computer simulation and is discussed in Sect. 3.2.

2.3 Joint FDE and Antenna Diversity Combining

After removal of GI from the received chip sequence $\{r_m(t);\ t = -N_g \sim N_c - 1\}$, N_c-point FFT is applied to decompose $\{r_m(t);\ t = 0 \sim N_c - 1\}$ into N_c subcarrier components $\{R_m(k);\ k = 0 \sim N_c - 1\}$. The kth subcarrier component $R_m(k)$ can be written as

$$R_m(k) = H_m(k)S(k) + N_m(k), \tag{3}$$

where $S(k)$, $H_m(k)$ and $N_m(k)$ are the kth subcarrier component of transmitted N_c-chip sequence $\{s(t);\ t = 0 \sim N_c - 1\}$, the channel gain and the noise component due to the AWGN, respectively. They are given by

$$\begin{cases} S(k) = \displaystyle\sum_{t=0}^{N_c-1} s(t) \exp\left(-j2\pi k \frac{t}{N_c}\right) \\ H_m(k) = \displaystyle\sum_{l=0}^{L-1} \xi_{l,m} \exp\left(-j2\pi k \frac{l}{N_c}\right) \\ N_m(k) = \displaystyle\sum_{t=0}^{N_c-1} \eta_m(t) \exp\left(-2\pi k \frac{t}{N_c}\right) \end{cases}, \tag{4}$$

where $E[|S(k)|^2] = 2E_cN_c/T_c$, $E[|H_m(k)|^2] = 1$ and $E[|N_m(k)|^2] = 2N_0N_c/T_c$.

Joint one-tap FDE and antenna diversity combining is carried out to obtain

$$\tilde{R}(k) = \sum_{m=0}^{N_r-1} R_m(k) w_m(k), \tag{5}$$

where $w_m(k)$ is the equalization weight. In this paper, we consider per-subcarrier one-tap MMSE equalization, MRC equalization and ZF equalization and compare their achievable BER performances in a frequency-selective Rayleigh fading channel in Sect. 3. The MRC equalization maximizes the signal-to-noise ratio (SNR) at each subcarrier but enhances the channel frequency-selectivity after equalization. The MMSE equalization minimizes the mean square error (MSE) between $S(k)$ and $\tilde{R}(k)$, while the ZF equalization gets $E[\tilde{R}(k)] = S(k)$ for all subcarriers (where the ensemble average operation is taken over noise samples).

MMSE weights for MC-CDMA are presented in Ref. [14] and succeeding literature, e.g., Refs. [6] and [7]. An extended work to jointly use the MMSE equalization and antenna diversity combining is presented for MC-CDMA in Ref. [15]. These results can be applied to DS-CDMA. Following the study on joint FDE and antenna diversity combining for MC-CDMA [15], the weights for DS-CDMA can be given by

$$w_m(k) = \begin{cases} \dfrac{H_m^*(k)}{\displaystyle\sum_{m=0}^{N_r-1} |H_m(k)|^2 + (E_c/N_0)^{-1}}, \text{ MMSE} \\ H_m^*(k), \text{ MRC} \\ \dfrac{H_m^*(k)}{\displaystyle\sum_{m=0}^{N_r-1} |H_m(k)|^2}, \text{ ZF} \end{cases}, \tag{6}$$

where E_c/N_0 is the average chip energy-to-AWGN power spectrum density ratio and * denotes the complex conjugate operation. We have assumed the perfect channel estimation.

Substitution of Eqs. (3) and (6) into Eq. (5) gives

$$\begin{aligned} \tilde{R}(k) &= S(k) \sum_{m=0}^{N_r-1} H_m(k) w_m(k) + \sum_{m=0}^{N_r-1} N_m(k) w_m(k) \\ &= S(k)\tilde{H}(k) + \tilde{N}(k), \end{aligned} \tag{7}$$

where $\tilde{H}(k)$ and $\tilde{N}(k)$ are the equivalent channel gain and noise after joint FDE and antenna diversity combining, respectively, and are given by

$$\begin{aligned} \tilde{H}(k) &= \sum_{m=0}^{N_r-1} H_m(k) w_m(k) \\ \tilde{N}(k) &= \sum_{m=0}^{N_r-1} N_m(k) w_m(k). \end{aligned} \tag{8}$$

$\tilde{N}(k)$ is a zero-mean complex Gaussian variable. As stated earlier, the MRC equalization enhances the frequency-selectivity of the channel after equalization. Using the ZF equalization, the frequency-nonselective channel can be perfectly restored after equalization (since we are assuming the ideal channel estimation), but the noise enhancement is produced at the subcarrier where the sum of the squared channel gains of N_r antennas drops. However, the MMSE equalization can avoid the noise enhancement by giving up the perfect restoration of the frequency-nonselective channel. The above is confirmed in Sect. 3.1.

2.4 Despreading

N_c-point IFFT is applied to $\{\tilde{R}(k); k = 0 \sim N_c - 1\}$ to obtain the time-domain chip sequence of $\{\tilde{r}(t); t = 0 \sim N_c - 1\}$:

$$\begin{aligned}\tilde{r}(t) &= \frac{1}{N_c}\sum_{k=0}^{N_c-1}\tilde{R}(k)\exp\left(j2\pi t\frac{k}{N_c}\right)\\ &= s(t)\left[\frac{1}{N_c}\sum_{k=0}^{N_c-1}\tilde{H}(k)\right]\\ &\quad+\left[\frac{1}{N_c}\sum_{k=0}^{N_c-1}\tilde{H}(k)\sum_{\substack{\tau=0\\ \neq t}}^{N_c-1}s(\tau)\exp\left(j2\pi(t-\tau)\frac{k}{N_c}\right)\right]\\ &\quad+\tilde{\eta}(t),\end{aligned} \tag{9}$$

where the first term represents the transmitted chip sequence and $\tilde{\eta}(t)$ is the noise samples at time t due to the AWGN, each characterized by the zero-mean complex Gaussian variable with a variance of

$$\sigma_{\tilde{\eta}}^2 = \frac{2N_0}{T_c}\left(\frac{1}{N_c}\sum_{k=0}^{N_c-1}\sum_{m=0}^{N_r-1}|w_m(k)|^2\right), \tag{10}$$

where $w_m(k)$ is given by Eq. (6). The second terms in Eq. (9) are the ICI components after FDE (which are called the residual ICI components); no ICI is produced for ZF equalization. Despreading is carried out on $\{\tilde{r}(t)\}$, giving

$$\tilde{d}(n) = \frac{1}{SF}\sum_{t=nSF}^{(n+1)SF-1}\tilde{r}(t)c^*(t), \tag{11}$$

which is the soft decision value for succeeding data demodulation on $d(n)$.

2.5 Matched Filter Bound

Neglecting the residual ICI resulting from IPI, the instantaneous signal-to-noise power ratio (SNR) γ for MRC equalization after despreading is given, from Eqs. (6), (8), (9)–(11), by

$$\gamma = 2\Gamma\frac{1}{N_c}\sum_{m=0}^{N_r-1}\sum_{k=0}^{N_c-1}|H_m(k)|^2 \tag{12}$$

for the given set of $\{H_m(k); k = 0 \sim N_c-1$ and $m = 0 \sim N_r-1\}$ or $\{\xi_{l,m}; l = 0 \sim L-1$ and $m = 0 \sim N_r-1\}$, where

$$\Gamma = SF\left(\frac{E_c}{N_0}\right) \tag{13}$$

is the average symbol energy-to-AWGN power spectrum density ratio E_s/N_0. Using Eq. (4), we have

$$|H_m(k)|^2 = \sum_{l=0}^{L-1}\sum_{l'=0}^{L-1}\xi_{l,m}\xi_{l',m}^*\exp\left(-j2\pi k\frac{l-l'}{N_c}\right) \tag{14}$$

and since

$$\frac{1}{N_c}\sum_{k=0}^{N_c-1}\exp\left(-j2\pi k\frac{l-l'}{N_c}\right) = \begin{cases}1 & \text{if } l = l'\\ 0 & \text{otherwise}\end{cases}, \tag{15}$$

we have

$$\frac{1}{N_c}\sum_{k=0}^{N_c-1}|H_m(k)|^2 = \sum_{l=0}^{L-1}|\xi_{l,m}|^2. \tag{16}$$

Hence, Eq. (12) can be rewritten as

$$\gamma = 2\Gamma\sum_{m=0}^{N_r-1}\sum_{l=0}^{L-1}|\xi_{l,m}|^2, \tag{17}$$

which is the sum of SNRs of the signals received via all paths and is equal to the SNR of matched filter (MF) output. Since we are neglecting the residual ICI, the following conditional BER gives the MF bound of MRC equalization [4]:

$$p_{\text{b,MF bound}}(\gamma) = \frac{1}{2}erfc\sqrt{\frac{\gamma}{2}}, \tag{18}$$

where binary phase shift keying (BPSK) data modulation is assumed. It should be also noted that Eq. (18) gives the coherent rake combiner output SNR when the IPI is neglected [16].

Assuming each path being subject to independent Rayleigh fading, the probability density function (pdf) of γ is given by [4]

$$p(\gamma) = \begin{cases}\dfrac{1}{(L-1)!\,(\Gamma/L)^L}\left(\dfrac{\gamma}{2}\right)^{L-1}\exp\left(-\dfrac{\gamma}{2\Gamma/L}\right), \\ \quad\text{if } \Gamma_l = \dfrac{\Gamma}{L} \text{ for all } l \\ \displaystyle\sum_{l=0}^{L-1}\frac{\pi_l}{\Gamma_l}\exp\left(-\frac{\gamma}{2\Gamma_l}\right), \text{ if } \Gamma_l \neq \Gamma_{l'} \text{ for } l \neq l'\end{cases}, \tag{19}$$

where $\Gamma_l = \Gamma E[|\xi_{l,m}|^2]$ for all m and π_l is defined as [4]

$$\pi_l = \prod_{\substack{l'=0\\ \neq l}}^{L-1}\frac{\Gamma_l}{\Gamma_l - \Gamma_{l'}}. \tag{20}$$

The first equation in Eq. (19) corresponds to the uniform power delay profile case and the second equation corresponds to the non-uniform power delay profile case, e.g., an exponential profile. The MF bounded average BER is therefore given by [4]

$$\begin{aligned}P_{\text{b,MF bound}}(\Gamma) &= \int_0^\infty p_{\text{b,MF bound}}(\gamma)p(\gamma)d\gamma\\ &= \begin{cases}\left[\dfrac{1}{2}\left(1-\sqrt{\dfrac{\Gamma}{\Gamma+L}}\right)\right]^L\displaystyle\sum_{k=0}^{L-1}\binom{L-1+k}{k} \\ \quad\left[\dfrac{1}{2}\left(1+\sqrt{\dfrac{\Gamma}{\Gamma+L}}\right)\right]^k, \\ \quad\text{if } \Gamma_l = \dfrac{\Gamma}{L} \quad \text{for all } l \\ \dfrac{1}{2}\displaystyle\sum_{l=0}^{L-1}\pi_l\left(1-\sqrt{\frac{\Gamma_l}{\Gamma_l+1}}\right), \text{if } \Gamma_l \neq \Gamma_{l'} \text{ for } l \neq l'\end{cases}\end{aligned}, \tag{21}$$

where $\begin{pmatrix} a \\ b \end{pmatrix}$ is the binomial coefficient. An approximate expression for the MF bounded average BER can be obtained for $\Gamma_l \gg 1$ using [4]

$$\sum_{k=0}^{L-1} \begin{pmatrix} L-1+k \\ k \end{pmatrix} = \begin{pmatrix} 2L-1 \\ L \end{pmatrix}. \tag{22}$$

We have

$$P_{\mathrm{b,MF\,bound}}(\Gamma) \approx \begin{cases} \dfrac{1}{\Gamma^L}\left(\dfrac{L}{4}\right)^L \begin{pmatrix} 2L-1 \\ L \end{pmatrix}, & \text{if } \Gamma_l = \dfrac{\Gamma}{L} \text{ for all } l \\ \dfrac{1}{\Gamma^L} \dfrac{\begin{pmatrix} 2L-1 \\ L \end{pmatrix}}{4^L \prod_{l=0}^{L-1}\left(\dfrac{\Gamma_l}{\Gamma}\right)}, & \text{if } \Gamma_l \neq \Gamma_{l'} \text{ for } l \neq l' \end{cases}. \tag{23}$$

Equation (23) shows that the FDE can achieve an L-th order frequency diversity effect if the residual ICI effect can be neglected. However, if the residual ICI effect is not neglected, the achievable BER performance degrades. The performance degradation may be severer with MRC equalization than with MMSE equalization.

2.6 Residual ICI

So far, we have assumed the single-code transmission. Here, we consider the residual ICI for both single-code and multi-code transmissions. When multi-code transmission is applied, the chip sequence (corresponding to Eq. (1)) is given by

$$s(t) = \sqrt{\frac{2E_c}{T_c}} \left[\sum_{i=0}^{C-1} d_i\left(\lfloor t/SF \rfloor\right) c_i(t \bmod SF) \right] c_{scr}(t), \tag{24}$$

where C is the multiplexing order, $\{c_i(t);\ t = 0 \sim SF-1\}$ is the orthogonal spreading chip sequence, and $\{c_{scr}(t);\ t = 0 \sim N_c - 1\}$ is a scramble sequence used for making the resulting multi-code signal white noise-like. Using Eq. (9), the despreader output for the ith symbol (corresponding to Eq. (11)) is given by

$$\tilde{d}(n) = \sqrt{\frac{2E_c}{T_c}} \left(\frac{1}{N_c} \sum_{k=0}^{N_c-1} \tilde{H}(k) \right) d_i(n) + \mu_{ICI}(n) + \mu_{noise}(n), \tag{25}$$

where the first term represents the desired data symbol component and the second and third terms are the residual ICI and noise due to AWGN, respectively. μ_{ICI} and μ_{noise} are given by

$$\mu_{ICI}(n) = \frac{1}{SF} \sum_{t=nSF}^{(n+1)SF-1} c^*(t) \times \frac{1}{N_c} \sum_{k=0}^{N_c-1} \tilde{H}(k) \left[\sum_{\substack{\tau=0 \\ \neq t}}^{N_c-1} s(\tau) \exp\left(j2\pi k \frac{t-\tau}{N_c} \right) \right]$$

$$\mu_{noise}(n) = \frac{1}{SF} \sum_{t=nSF}^{(n+1)SF-1} c^*(t) \times \frac{1}{N_c} \sum_{k=0}^{N_c-1} \tilde{N}(k) \exp\left(j2\pi t \frac{k}{N_c} \right), \tag{26}$$

where

$$c(t) = c_i(t \bmod SF) c_{scr}(t). \tag{27}$$

The residual ICI can be approximated as a zero-mean Gaussian process. Since the multi-code DS-CDMA signal using the scramble sequence is white-noise like, i.e., $E[s(\tau)s^*(\tau')] = (2E_cC/T_c)\delta(\tau-\tau')$ with $\delta(t)$ being the delta function, we can show that the variance of μ_{ICI} is given by (for the sake of brevity, derivation is not shown here)

$$\sigma_{ICI}^2 = \frac{1}{2}E[|\mu_{ICI}|^2] = \frac{E_c}{T_c}\frac{1}{SF_{eq}} \left[\frac{1}{N_c} \sum_{k=0}^{N_c-1} \left| \tilde{H}(k) \right|^2 - \left| \frac{1}{N_c} \sum_{k=0}^{N_c-1} \tilde{H}(k) \right|^2 \right], \tag{28}$$

where $SF_{eq} = SF/C$ is the equivalent spreading factor (the special case is SF_{eq}=SF for the single-code transmission). It can be understood from Eq. (28) that the ICI variance is proportional to SF_{eq}. Note that if both single-code and multi-code transmissions use the same SF_{eq} for the given chip rate, they provide the same data rate. Therefore, for the same data rate, the same BER performance can be achieved with the single-code and multi-code transmissions. This is confirmed by the computer simulation in Sect. 3.

3. Computer Simulation

The simulation parameters are summarized in Table 1. We assume BPSK data modulation, the FFT window size of N_c=256 chips and the GI of N_g=32 chips. Fading channel is assumed to be a frequency-selective fading channel having an L-path exponential power delay profile with decay factor α (i.e., $\Gamma_l = \alpha^l \Gamma_0$ for $l = 1 \sim L-1$). Perfect chip timing and ideal channel estimation are assumed. First, we consider the single-code and single-user case and compare the BER performances achievable with MMSE, MRC and ZF equalizations. How the fading rate and the spreading factor affect the BER performance is also evaluated. Furthermore, the BER performance comparison between FDE and rake combining is presented for various values of SF and also performance comparison between multi-code DS-CDMA and single-code DS-CDMA, both using FDE, is presented. Finally, we extend our evaluation to the multi-user case. Both downlink and uplink are considered and how the BER performances of downlink and uplink differ is discussed. As a spreading sequence, a pseudo-noise (PN) sequence with a repetition of 4095 chips is used for the uplink case while the product of Walsh sequence and the PN sequence is used for the downlink [3].

Table 1 Simulation parameters.

Transmitter	Modulation	BPSK
	Number of FFT points	N_c=256
	GI	N_g=32(chip)
	Spreading sequence	Product of Walsh sequence and PN sequence (downlink) PN sequence (uplink)
	Spreading factor	SF=1~256
Channel	Fading	Frequency -selective Rayleigh fading
	Power delay profile	L=16-path exponential power delay profile
		Decay factor α=0, 8 dB
Receiver	Number of receive antennas	N_r=1, 2, 4
	Frequency-domain Equalization	MMSE, MRC, ZF
	Channel estimation	Ideal

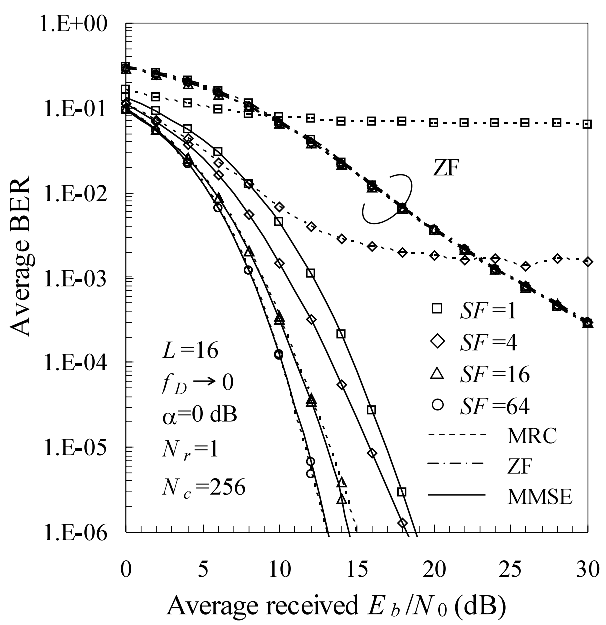

Fig. 3 Simulated BER performances of single-code DS-CDMA using MMSE, MRC, and ZF equalizations. Single-user case. No antenna diversity (N_r=1), L=16, $f_D \to 0$ and α=0 dB.

3.1 Comparison of MMSE, MRC and ZF Equalizations

The simulated BER performances of single-code DS-CDMA with MMSE, MRC and ZF equalizations are plotted for comparison in Fig. 3 as a function of the average received bit energy-to-AWGN noise power spectrum density ratio E_b/N_0, given by $E_b/N_0 = SF(1 + N_g/N_c)(E_c/N_0)$, for the case of no antenna diversity ($N_r = 1$), L=16, $f_D \to 0$ and α=0 dB. It can be seen from the figure that the ZF equalization gives the same BER performance for all SF values since the frequency-nonselective channel is perfectly restored. The BER floors are seen with MRC equalization for SF=1 and 4, due to the large ICI produced by the enhanced frequency-selectivity. When SF=16 and 64, however, the MRC equalization can achieve almost the same BER performance as MMSE equalization since the residual ICI can be sufficiently suppressed by the despreading process. On the other hand, the MMSE equalization always achieves the best BER performance. It should be noted that this result is different from the MC-CDMA case. In MC-CDMA, it is well-known [6] that for the single-user case, MRC equalization provides the best performance. The reason for this is that in DS-CDMA, the transmitted symbol energy is spread over the entire signal bandwidth and hence, MRC equalization produces large ICI or self-interference due to the enhancement of the frequency-selectivity (however in MC-CDMA, the self-interference is not produced). Hence, in the following, we use the MMSE equalization only.

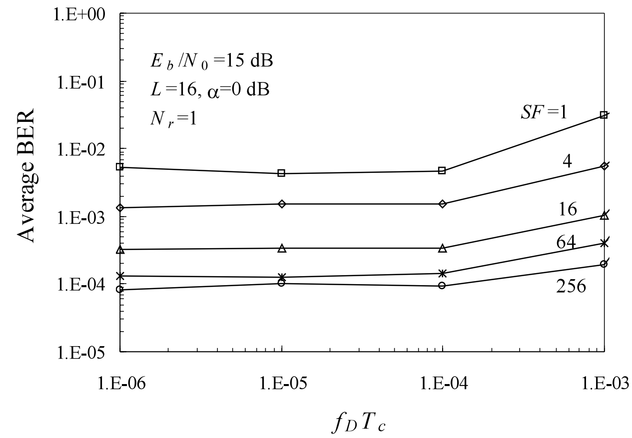

Fig. 4 Dependency of the BER on the maximum Doppler frequency $f_D T_c$ at the average E_b/N_0=15 dB.

3.2 Impact of Fading Rate

So far, we have assumed block fading, where the path gains stay constant over one data frame (the frame length in time equals $(N_c + N_g)T_c$). However, in practice, path gains may vary during one frame if the mobile station travels fast. It is interesting to see the impact of the fading maximum Doppler frequency f_D on the achievable BER performance, where f_D is given by the traveling speed/carrier wavelength [1]. The BER dependency on $f_D T_c$ at the average E_b/N_0=15 dB is plotted in Fig. 4 for the single receive antenna case. It can be seen that the achievable BER is almost insensitive to $f_D T_c$ if $f_D T_c < 0.0001$ when N_c=256 (this corresponds to the traveling speed of 200 km/h for the chip rate ($1/T_c$) of 10 Mcps and 5 GHz carrier frequency). Hence, block fading is assumed in the following simulations.

3.3 Comparison of MMSE Equalization and Rake Combining

Figure 5 plots the average BER performances of single-code DS-CDMA using MMSE equalization and those using rake combining with *SF* as a parameter for α=0 dB (strong frequency-selectivity) and 8 dB (weak frequency-selectivity) when $f_D \to 0$. It is seen from the figure that, using small *SF* values (e.g., *SF*=1 and 4), MMSE equalization provides better BER performance than rake combining; BER floors are seen using rake combining due to strong IPI, but no BER floors are seen using MMSE equalization. Notice that BER floors when α=8 dB are smaller than when $\alpha = 0$ dB due to less IPI. However, it should be noted that using large *SF* (e.g., *SF*=64), rake combining can effectively suppress the IPI and thus, achieves slightly better BER performance than MMSE equalization. This slight performance inferiority of about 0.5 dB in the required E_b/N_0 observed in the MMSE equalization is due to the power loss resulting from the GI insertion. An improved BER performance achieved when α=0 dB compared to the case when α=8 dB is due to the effect of increased frequency diversity (increased path diversity) for MMSE equalization (rake combining). The reduction in the required E_b/N_0 for achieving BER=10^{-4} when α=0 dB from the case when α=8 dB is as much as about 8.5 dB.

Also plotted in Fig. 5 are the MF bound BER performances computed using Eq. (21). The average BER performance with MMSE equalization approaches the MF bound as *SF* becomes large. When *SF*=4, the E_b/N_0 degradation for achieving BER=10^{-4} is 4 (3) dB for MMSE equalization in the case of α=0 (8) dB. When *SF*=16, it becomes as small as 1.7 (0.7) dB in the case of α=0 (8) dB.

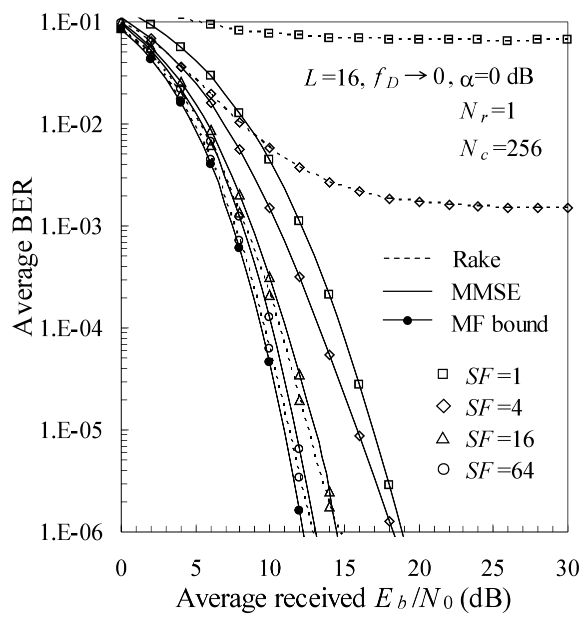

(a) α=0 dB.

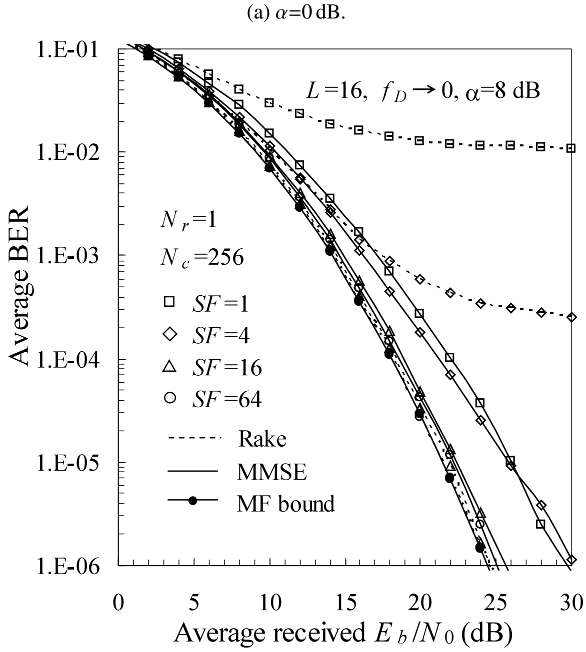

(b) α=8 dB.

Fig. 5 Simulated average BER performances of single-code DS-CDMA using MMSE equalization and using rake combining with *SF* as a parameter for α=0 and 8 dB. Single-user case. No antenna diversity (N_r=1) and $f_D \to 0$.

3.4 Joint MMSE Equalization and Antenna Diversity Combining

The simulated BER performances using joint MMSE equalization and antenna diversity combining are plotted in Fig. 6 with the number N_r of diversity antennas and the spread-

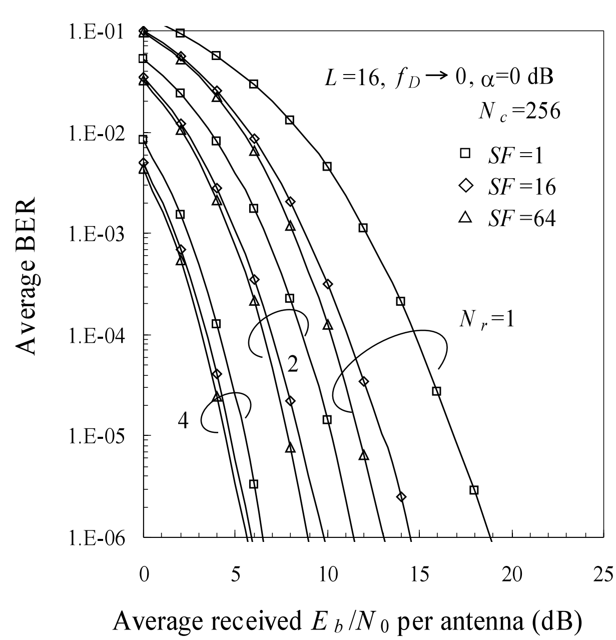

Fig. 6 Simulated BER performance of single-code DS-CDMA using joint MMSE equalization and antenna diversity combining with the number N_r of diversity antennas and the spreading factor *SF* as parameters when α=0 dB. Single-user case.

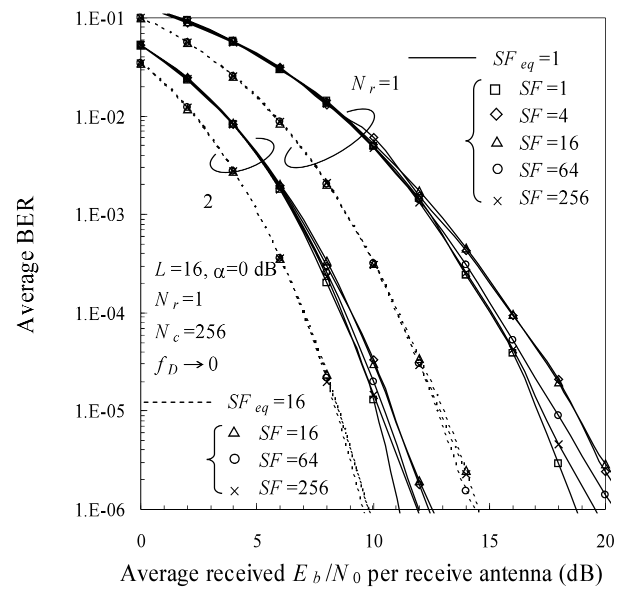

Fig. 7 Simulated BER performance of single-code and multicode DS-CDMA when SF_{eq}=1 and 16. Single-user case.

ing factor SF as parameters when α=0. It can be clearly seen that the use of antenna diversity combining is always beneficial irrespective of SF. When SF=64, an antenna diversity gain of as much as about 7 dB can be achieved for a BER=10^{-4} by the use of N_r=4-branch antenna diversity combining.

3.5 Performance Comparison of Single-Code DS-CDMA and Multi-Code DS-CDMA

So far we have considered the single-code DS-CDMA. It is seen in Fig. 3 that the BER performance improves as SF increases and the required E_b/N_0 value for achieving BER=10^{-4} can be reduced by about 4.5 dB when SF=64 compared to the case of SF=1. Using SF=1 is equivalent to the nonspread SC transmission. Hence, the DS-CDMA with MMSE equalization can achieve better BER performance by reducing the data rate or increasing the bandwidth for the same data rate. It is interesting to compare the BER performances of single-code and multi-code transmissions for the same data rate at the same chip rate (i.e., for the same equivalent spreading factor SF_{eq}). Figure 7 plots the simulated BER performances of single-code and multi-code DS-CDMA when SF_{eq}=1 and 16. It can be seen that the BER performance of single-code DS-CDMA is almost the same as that of multi-code DS-CDMA for the same SF_{eq}. This is because if SF_{eq} is the same, the variance of residual ICI is the same for the single-code and multi-code transmissions, as discussed in Sect. 2.6.

3.6 Multi-Rate and Multi-User Environment

In the previous subsections, we have discussed the performance improvement achievable with FDE for the case of single-user. Here, we assume single-code transmission (i.e., C=1) and consider the uplink and downlink when U users are simultaneously communicating with a base station at different data rates. Joint MMSE equalization and N_r-branch antenna diversity combining is considered. Without loss of generality, u=0th user is assumed to be the desired user. The k-th subcarrier component $R_m(k)$ obtained by the FFT operation, which corresponds to Eq. (3) for the single-user case, can be given by

$$R_m(k) = \begin{cases} H_m^{(0)}(k)S^{(0)}(k) + \sum_{u=1}^{U-1} H_m^{(u)}(k)S^{(u)}(k) + N_m(k) \\ \quad \text{for uplink} \\ H_m(k)\sum_{u=0}^{U-1} S^{(u)}(k) + N_m(k) \\ \quad \text{for downlink} \end{cases}, \tag{29}$$

where the superscript u denotes the user index (u=0$\sim$ $U-1$) and $S^{(u)}(k)$ is the k-th subcarrier component of u-th user's chip sequence. For the uplink case, the first term in Eq. (29) represents the desired user's signal component and the second represents the multi-user interference (MUI) from $U-1$ interfering users.

For the downlink case, all users' spread signals are synchronous and go through the same propagation channel. Hence, $H_m^{(u)}(k) = H_m(k)$ for all u. For the downlink, as understood from Fig. 7 (different spreading code is assigned to different user), orthogonal spreading codes can be used to multiplex as many users as the spreading factor $SF^{(u)}$ of u-th user. In this paper, orthogonal variable spreading factor (OVSF) codes of length $SF^{(u)}$ chips are used ($SF^{(u)}$ is equal to an integer power of 2) and a PN sequence used in the single-user case is used as a common scramble sequence.

To derive the MMSE weights, we first define the equalization error. For the uplink case, each user's spread signal goes through a different channel, we use $S^{(0)}(k)$ as the reference. On the other hand, for the downlink case, all users' signals go through the same channel, we use $\sum_{u=0}^{U-1} S^{(u)}(k)$ as the reference. From Eq. (29), the equalization error at the kth subcarrier is given by

$$\begin{aligned} \varepsilon(k) &= \sum_{m=0}^{N_r-1} w_m(k)R_m(k) - S^{(0)}(k) \\ &= \left\{\sum_{m=0}^{N_r-1}\sum_{u=0}^{U-1} w_m(k)H_m^{(u)}(k)S^{(u)}(k)\right\} \\ &\quad + \sum_{m=0}^{N_r-1} w_m(k)N_m(k) - S^{(0)}(k) \text{ for uplink} \\ \varepsilon(k) &= \sum_{m=0}^{N_r-1} w_m(k)R_m(k) - \sum_{u=0}^{U-1} S^{(u)}(k) \\ &= \left\{\sum_{u=0}^{U-1} S^{(u)}(k) \sum_{m=0}^{N_r-1} w_m(k)H_m(k)\right\} \end{aligned}$$

$$+\sum_{m=0}^{N_r-1} w_m(k)N_m(k) - \sum_{u=0}^{U-1} S^{(u)}(k)$$
$$\text{for downlink.} \tag{30}$$

The set of MMSE weights $\{w_m(k); m = 0 \sim N_r - 1\}$ is the one that minimizes the mean square error (MSE) $E[|\varepsilon(k)|^2]$ for the given set of $\{H_m^{(u)}(k); m = 0 \sim N_r - 1\}$, i.e., $\partial E[|\varepsilon(k)|^2]/\partial w_m(k) = 0$ for all m. Since $E[|S^{(u)}(k)|^2] = (2E_s/T_c)N_c/SF^{(u)}$ (this can be found from Eqs. (1) and (4)) and since $N_m(k)$ is a zero-mean complex-valued noise having variance $2(N_0/T_c)N_c)$, the MSE for the given set of $\{H_m^{(u)}(k); m = 0 \sim N_r - 1\}$ becomes

$$E[|\varepsilon(k)|^2] = \begin{cases} \dfrac{2E_s}{T_c}\dfrac{N_c}{SF^{(0)}} \left[\begin{array}{l} 1 + \displaystyle\sum_{u=0}^{U-1} \frac{SF^{(0)}}{SF^{(u)}} \left| \sum_{m=0}^{N_r-1} w_m(k) H_m^{(u)}(k) \right|^2 \\ -2\mathrm{Re}\left[\displaystyle\sum_{m=0}^{N_r-1} w_m(k) H_m^{(0)}(k) \right] \\ +\left(\dfrac{E_s}{SF^{(0)} N_0} \right)^{-1} \displaystyle\sum_{m=0}^{N_r-1} |w_m(k)|^2 \end{array} \right] \\ \text{for uplink} \\ \displaystyle\sum_{u=0}^{U-1} \frac{2E_s}{T_c}\frac{N_c}{SF^{(u)}} \left[\begin{array}{l} 1 + \left| \displaystyle\sum_{m=0}^{N_r-1} w_m(k) H_m(k) \right|^2 \\ -2\mathrm{Re}\left[\displaystyle\sum_{m=0}^{N_r-1} w_m(k) H_m(k) \right] \\ +\left(\displaystyle\sum_{u=0}^{U-1} \frac{1}{SF^{(u)}} \frac{E_s}{N_0} \right)^{-1} \\ \times \displaystyle\sum_{m=0}^{N_r-1} |w_m(k)|^2 \end{array} \right] \\ \text{for downlink} \end{cases} . \tag{31}$$

Following [15], we can obtain the following MMSE weight:

$$w_m(k) = \begin{cases} \dfrac{H_m^{(0)*}(k)}{\displaystyle\sum_{u=0}^{U-1} \frac{1}{SF^{(u)}} \sum_{m=0}^{N_r-1} |H_m^{(u)}(k)|^2 + \left(\frac{E_s}{N_0} \right)^{-1}} \\ \quad \text{for uplink} \\ \dfrac{H_m^*(k)}{\left(\displaystyle\sum_{u=0}^{U-1} \frac{1}{SF^{(u)}} \right) \left(\sum_{m=0}^{N_r-1} |H_m(k)|^2 \right) + \left(\frac{E_s}{N_0} \right)^{-1}} \\ \quad \text{for downlink} \end{cases} . \tag{32}$$

The equivalent spreading factor SF_{eq} for the multi-rate and multi-user case is given by $SF_{eq} = 1/\sum_{u=0}^{U-1}(1/SF^{(u)})$. Figure 8 plots the simulated BER performances of the downlink, for the multi-rate and multi-user case with the equivalent spreading factor SF_{eq}=4 and 1 when N_r=2. We assume two groups of users with different data rates using SF=16 and 64, respectively. For comparison, the BER performance for the single-rate case, but with the same equivalent spreading factor ($SF_{eq} = SF/U$ for the single-rate case) is also plotted. The BER performance for ideal rake combining is also plotted. MMSE equalization provides much better performance than rake combining, while rake combining produces BER floors due to MUI resulting from large IPI. With MMSE equalization, the BER performance is almost the same for the single-rate and multi-rate cases as far as SF_{eq} is equal. The BER performance with SF_{eq}=1 slightly degrades compared to SF_{eq}=4 due to the increased MUI resulting from IPI; however no BER floors are seen as for the rake combining. The above simulation results confirm that rake combining can be replaced by MMSE equalization with much improved performance on the downlink.

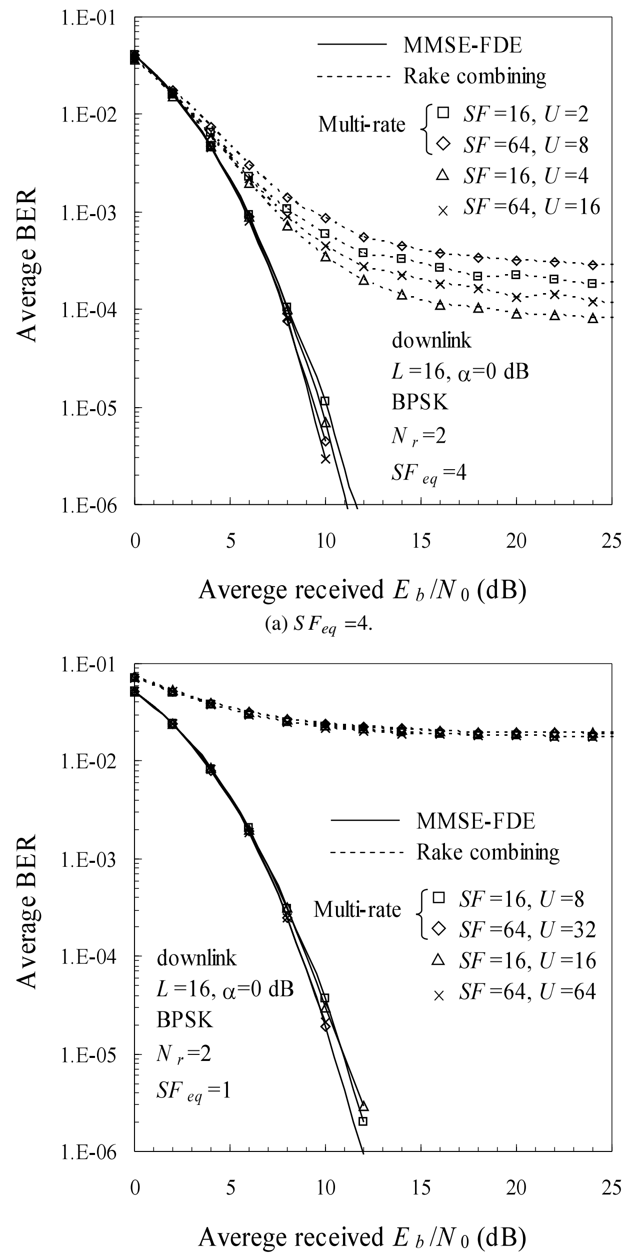

(a) SF_{eq} =4.
(b) SF_{eq}=1.

Fig. 8 Downlink BER performance in multi-rate and multi-user environment.

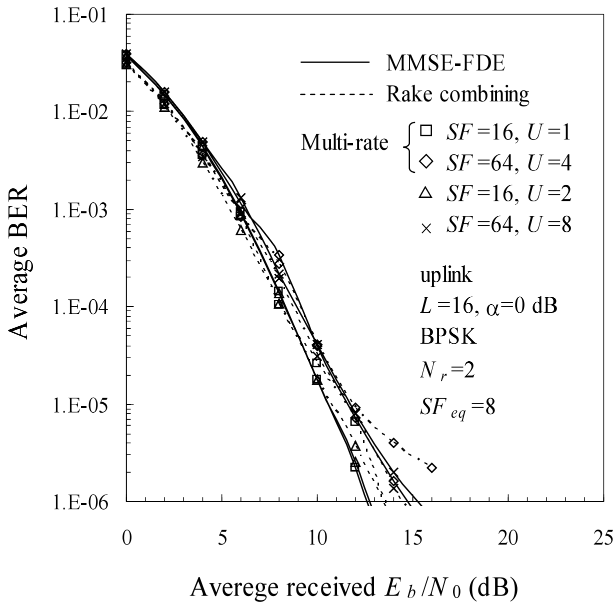

(a) SF_{eq}=8.

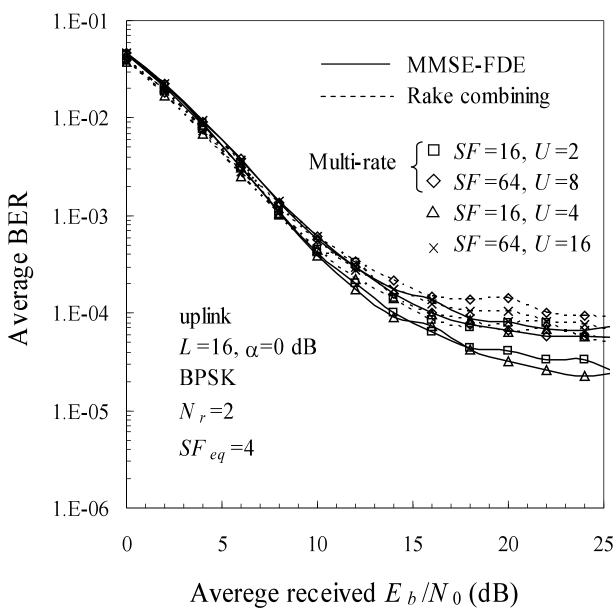

(b) SF_{eq}=4.

Fig. 9 Uplink BER performance in multi-rate and multi-user environment.

Figure 9 plots the simulated BER performances of the uplink, for the multi-rate and multi-user case with the equivalent spreading factor SF_{eq}=8 and 4 when N_r=2. In the case of uplink, since different user's signal goes through a different fading channel and furthermore their transmitting timings are asynchronous, BER floors are seen due to large MUI for both MMSE equalization and rake combining. This indicates that an MUI cancellation technique must be adopted for improving the uplink BER performance. The study of MUI is left as a future study.

4. Conclusion

In this paper, joint frequency-domain equalization and antenna diversity combining was presented for the reception of multi-rate DS-CDMA signals and the achievable BER performance in a frequency-selective Rayleigh fading channel was evaluated by computer simulation. Assuming the single-code and single-user case, the BER performances using MMSE, MRC and ZF equalizations were compared to find that the MMSE equalization gives the best BER performance unlike MC-CDMA. Also found was that as the spreading factor *SF* increases, the MMSE equalization improves the BER performance since the ICI produced by the channel frequency-selectivity can be effectively suppressed. When a small spreading factor is used (e.g., *SF*=1 and 4) for high speed data transmissions, the BER floors appear when rake combining is used; however, no BER floor is produced when MMSE equalization is applied. When *SF* is large enough (e.g., *SF*=64), however, BER performances for rake combining and MMSE equalization are almost the same. Performance evaluation in the multi-rate and multi-user case showed that the rake combining can be replaced by the MMSE equalization with much improved downlink performance, but the uplink performance is almost the same for MMSE equalization and rake combining. This indicates that an MUI cancellation technique must be adopted for improving the uplink BER performance. The mathematical expressions for the despread signal and the residual ICI after FDE, derived in this paper, may be useful for the theoretical BER analysis and the study of ICI cancellation technique.

In this paper, ideal channel estimation was assumed to compute the equalization weights. In practical systems, pilot-assisted channel estimation can be used [17]. The use of pilot-assisted channel estimation in a time-selective fading degrades the achievable BER performance with MMSE equalization. This is an interesting future study.

References

[1] F. Adachi, "Wireless past and future—Evolving mobile communications systems," IEICE Trans. Fundamentals, vol.E83-A, no.1, pp.55–60, Jan. 2001.
[2] W.C. Jakes Jr., ed., Microwave mobile communications, Wiley, New York, 1974.
[3] F. Adachi, M. Sawahashi, and H. Suda, "Wideband DS-CDMA for next generation mobile communications systems," IEEE Commun. Mag., vol.36, no.9, pp.56–69, Sept. 1998.
[4] J.G. Proakis, Digital communications, 3rd ed., McGraw-Hill, 1995.
[5] F. Adachi, "Effects of orthogonal spreading and Rake combining on DS-CDMA forward link in mobile radio," IEICE Trans. Commun., vol.E80-B, no.11, pp.1703–1712, Nov. 1997.
[6] S. Hara and R. Prasad, "Overview of multicarrier CDMA," IEEE Commun. Mag., vol.35, no.12, pp.126–144, Dec. 1997.
[7] S. Hara and R. Prasad, "Design and performance of multicarrier CDMA system in frequency-selective Rayleigh fading channels," IEEE Trans. Veh. Technol., vol.48, no.5, pp.1584–1595, Sept. 1999.
[8] L. Hanzo, W. Webb, and T. Keller, Single- and multi-carrier quadrature amplitude modulation, John Wiley & Sons, 2000.
[9] M. Helard, R. Le Gouable, J.-F. Helard, and J.-Y. Baudais, "Multi-

carrier CDMA techniques for future wideband wireless networks," Ann. Telecommun., vol.56, pp.260–274, 2001.
[10] H. Atarashi and M. Sawahashi, "Variable spreading orthogonal frequency and code division multiplexing (VSF-OFCDM) for broadband packet wireless access," IEICE Trans. Commun., vol.E86-B, no.1, pp.291–299, Jan. 2003.
[11] T. Sao and F. Adachi, "Comparative study of various frequency equalization techniques for dounlink of a wireless OFDM-CDMA system," IEICE Trans. Commun., vol.E86-B, no.1, pp.352–364, Jan. 2003.
[12] D. Falconer, S.L. Ariyavisitakul, A. Benyamin-Seeyar, and B. Eidson, "Frequency domain equalization for single-carrier broadband wireless systems," IEEE Commun. Mag., vol.40, no.4, pp.58–66, April 2002.
[13] F. Adachi, T. Sao, and T. Itagaki, "Performance of multicode DS-CDMA using frequency domain equalization in a frequency selective fading channel," Electron. Lett., vol.39, pp.239–241, Jan. 2003.
[14] A. Chouly, A. Brajal, and S. Jourdan, "Orthogonal multicarrier techniques applied to direct sequence spread spectrum CDMA system," Proc. IEEE Globecom'93, pp.1723–1728, Nov. 1993.
[15] F. Adachi and T. Sao, "Joint antenna diversity and frequency-domain equalization for multi-rate MC-CDMA," IEICE Trans. Commun., vol.E86-B, no.11, pp.3217–3224, Nov. 2003.
[16] F. Adachi, "Time- and frequency-domain expressions for Rake combiner output SNR," IEICE Trans. Commun., vol.E85-B, no.1, pp.340–342, Jan. 2002.
[17] H. Andoh, M. Sawahashi, and F. Adachi, "Channel estimation filter using time-multiplexed pilot channel for coherent RAKE combining in DS-CDMA mobile radio," IEICE Trans. Commun., vol.E81-B, no.7, pp.1517–1526, July 1998.

Kazuaki Takeda received his B.E. and M.S. degrees in communications engineering from Tohoku University, Sendai, Japan, in 2003 and 2004. Currently he is a PhD student at the Department of Electrical and Communications Engineering, Graduate School of Engineering, Tohoku University. His research interests include frequency-domain equalization for direct sequence CDMA and transmit/receive diversity techniques.

Fumiyuki Adachi received the B.S. and Dr. Eng. degrees in electrical engineering from Tohoku University, Sendai, Japan, in 1973 and 1984, respectively. In April 1973, he joined the Electrical Communications Laboratories of Nippon Telegraph & Telephone Corporation (now NTT) and conducted various types of research related to digital cellular mobile communications. From July 1992 to December 1999, he was with NTT Mobile Communications Network, Inc. (now NTT DoCoMo, Inc.), where he led a research group on wideband/broadband CDMA wireless access for IMT-2000 and beyond. Since January 2000, he has been with Tohoku University, Sendai, Japan, where he is a Professor of Electrical and Communication Engineering at the Graduate School of Engineering. His research interests are in CDMA wireless access techniques, equalization, transmit/receive antenna diversity, MIMO, adaptive transmission, and channel coding, with particular application to broadband wireless communications systems. From October 1984 to September 1985, he was a United Kingdom SERC Visiting Research Fellow in the Department of Electrical Engineering and Electronics at Liverpool University. He was a co-recipient of the IEICE Transactions best paper of the year award 1996 and again 1998 and also a recipient of Achievement award 2003. He is an IEEE Fellow and was a co-recipient of the IEEE Vehicular Technology Transactions best paper of the year award 1980 and again 1990 and also a recipient of Avant Garde award 2000.